Zirconium-91 Chemical Shifts and Line Widths as Indicators of Coordination Geometry Distortions in Zirconocene Complexes†

Michael Bühl,* Gudrun Hopp, and Wolfgang von Philipsborn*

Organisch-chemisches Institut, Universität Zürich, CH-8057 Zürich, Switzerland

Stefan Beck, Marc-Heinrich Prosenc, Ursula Rief, and Hans-Herbert Brintzinger*

Fakultät für Chemie, Universität Konstanz, D-78464 Konstanz, Germany

Received September 25, 1995⊗

^{91}Zr NMR chemical shifts and line widths ($\Delta\nu_{1/2}$) are reported for a number of ring-bridged and ring-substituted zirconocene dichloride, dibromide, and dimethyl complexes. Ab initio computations at the SCF level employing basis sets of moderate size suggest that the magnitude of the electric field gradient (EFG) at the Zr atom dominates $\Delta\nu_{1/2}$ when the substituents X at Zr are varied (X = Br, Cl, Me). Substituents at the cyclopentadiene (Cp) rings affect the computed EFGs much less; in these cases, the line widths $\Delta\nu_{1/2}$ are governed by the molecular correlation times τ_c, which were obtained for several zirconocene dichlorides from T_1(^{13}C) measurements. Experimental trends in δ(^{91}Zr) of zirconocenes are well reproduced computationally with the IGLO (individual gauge for localized orbitals) or GIAO (gauge including atomic orbitals) SCF methods employing large basis sets. Model calculations suggest that δ(^{91}Zr), as well as the EFG, are quite sensitive to the inclination and twist angles of the Cp rings and, to a lesser extent, to the CpZrCp′ angle. A substantial deshielding, δ(^{91}Zr) ca. 700 ppm, is predicted for $(C_5H_5)_2ZrMe^+$, presumably the active olefin-polymerizing catalyst.

Introduction

Relations between the structures of ring-bridged and ring-substituted zirconocene complexes and their properties as catalysts for olefin polymerization[2−5] and other C−C bond formation reactions[6−9] are of current interest. ^{91}Zr NMR spectroscopy has been used by several research groups[10−14] as a probe for the environment of the Zr centers in complexes of this type. Following initial studies by McGlinchey and co-workers,[13,14] Benn and Rufinska reported ^{91}Zr NMR spectra for a number of $(C_5H_5)_2$Zr(diene) complexes and proposed that the ^{91}Zr chemical shifts are related, through the paramagnetic shielding terms, to the optical excitation energies.[12,15] Siedle and co-workers have utilized ^{91}Zr NMR spectroscopy to identify cationic zirconocene species.[10] In a recent study, Böhme, Thiele, and Rufinska have reported ^{91}Zr NMR data for several ring-substituted and ring-bridged zirconocene dichloride compounds and have correlated the ^{91}Zr shifts with C_5-ring centroid−Zr−centroid angles in these complexes.[11]

The line widths $\Delta\nu_{1/2}$ of the ^{91}Zr resonances are conspicuously variable in different zirconocene complexes, ranging from very sharp peaks with $\Delta\nu_{1/2}$ = 18 Hz [$(C_5H_5)_2ZrBr_2$] to resonances several kHz wide in other complex species[10−15] or even signals undetectably broad, i.e. $\Delta\nu_{1/2}$ > ca. 10 kHz. These large and variable line widths represent a serious obstacle for quantitative ^{91}Zr NMR studies and sometimes even for the detection of individual zirconocene complex species.[10] On the other hand, Hafner and co-workers have reported that ^{49}Ti NMR line widths for (C_5H_5)Ti$(OR)_2$(allyl) complexes with different carbohydrate ligands are a very useful indicator for their structural flexibility and, as a consequence, for their effectiveness in inducing stereoselective aldol reactions.[16] We have thought it worthwhile to investigate how ^{91}Zr NMR parameters of typical zirconocene complexes depend on their coordination geometries and, therefore, determined the ^{91}Zr chemical shifts and line widths of a series of zirconocene complexes. Ab initio calculations have been performed of the electric field gradients (EFGs) of $(C_5H_5)_2ZrX_2$ species (X = Br, Cl, Me). Further computations have been carried out for substituted and for artificially distorted

† Transition Metal NMR Spectroscopy. 29. Part 28: see ref 1.

‡ E-mail: buehl@oci.unizh.ch.
§ E-mail: beck@chclu.chemie.uni-konstanz.de.

⊗ Abstract published in *Advance ACS Abstracts,* January 1, 1996.

(1) Asaro, F.; Costa, G.; Dreos, R.; Pellizer, G.; von Philipsborn, W. *J. Organomet. Chem.*, in press.
(2) Möhring, P. C.; Coville, N. J. *J. Organomet. Chem.* **1994**, *479*, 1.
(3) Sinclair, K. B.; Wilson, R. B. *Chem. Ind.* **1994**, 857.
(4) Kaminsky, W. *Catal. Today* **1994**, *20*, 257.
(5) Brintzinger, H. H.; Fischer, D.; Mülhaupt, R.; Rieger, B.; Waymouth, R. M. *Angew. Chem., Int. Ed. Engl.* **1995**, *34*, 1143.
(6) Vostrikova, O. S.; Ibragimov, A. G.; Sultanov, R. M.; Dzhelimev, U. M. *Organomet. Chem. USSR* **1992**, *5*, 377.
(7) Morken, J. P.; Didiuk, M. T.; Hoveyda, A. H. *J. Am. Chem. Soc.* **1993**, *115*, 6997.
(8) Negishi, E. I.; Takahashi, T. *Acc. Chem. Res.* **1994**, *27*, 124.
(9) Knight, K. S.; Waymouth, R. M. *Organometallics* **1994**, *13*, 2575.
(10) Siedle, A. R.; Newmark, R. A.; Gleason, W. B.; Lamanna, W. M. *Organometallics* **1990**, *9*, 1290.
(11) Böhme, U.; Thiele, K. H.; Rufinska, A. *Z. Anorg. Allg. Chem.* **1994**, *620*, 1455.
(12) Benn, R.; Rufinska, A. *Angew. Chem.* **1984**, *98*, 851.
(13) Sayer, B. G.; Hao, N.; Dénès, G.; Bickley, D. G.; McGlinchey, M. J. *Inorg. Chim. Acta* **1981**, *48*, 53.
(14) Sayer, B. G.; Thompson, J. I. A.; Hao, N.; Birchall, T.; Eaton, D. R.; McGlinchey, M. J. *Inorg. Chem.* **1981**, *20*, 3748.
(15) Benn, R.; Rufinska, A. *J. Organomet. Chem.* **1984**, *273*, C51.
(16) Hafner, A.; Duthaler, R. O.; Marti, R.; Rihs, G.; Rothe-Streit, P.; Schwarzenbach, F. *J. Am. Chem. Soc.* **1992**, *114*, 2321.

0276-7333/96/2315-0778$12.00/0

zirconocenes in order to assess the geometric and electronic effects of substituents on the ^{91}Zr NMR line widths.

In addition, ^{91}Zr chemical shifts have been computed for some zirconocenes and for ZrX_6^{2-} (X = F, Cl) employing the IGLO[17−20] (individual gauge for localized orbitals) and GIAO[21−23] (gauge including atomic orbitals) methods. While computations of NMR chemical shifts are now routinely possible for the lighter, i.e. first- and second-row nuclei (both at SCF and at electron-correlated levels),[19,24−28] much less is known regarding the reliabilty of such calculations for compounds of heavier elements. It has recently been shown that electron correlation effects can be quite important in chemical shift computations for heavier nuclei, e.g., for Ga and Se compounds.[29−31] On the other hand, experimental trends for certain classes of compounds can often be reproduced quite satisfactorily at SCF level, even when fourth-row elements such as Mo, Cd, or Sn are involved.[32,33] As the SCF-based methods prove to perform rather well for ^{91}Zr NMR chemical shift calculations, interesting predictions of $\delta(^{91}Zr)$ values can be made for some cationic zirconocene complexes involved in the catalytic olefin polymerization process.

Experimental and Computational Section

1. Zirconocene Syntheses. The following zirconocene chloride complexes were prepared by previously described methods: $(C_5H_5)_2ZrCl_2$ **(1a)**,[34] $(C_5H_5)_2Zr(Cl)Me$ **(1d)**,[35] $(C_5Me_5)_2ZrCl_2$ **(2a)**,[36] $(C_5H_4Me)_2ZrCl_2$ **(3a)**,[37] $(C_5H_4{}^tBu)_2ZrCl_2$ **(4a)**,[38] $(C_5H_4SiMe_3)_2ZrCl_2$ **(5a)**,[39] $Me_4C_2(C_5H_4)_2ZrCl_2$ **(6a)**,[40] $Me_2Si(C_5H_4)_2ZrCl_2$ **(7a)**.[41,42] The dicyclohexyl-bridged complex $(C_5H_{10})_2C_2(C_5H_4)_2ZrCl_2$ **(8a)** was prepared in analogy to the corresponding titanium complex:[43] Reaction of the dimagnesium salt $(C_5H_{10})_2C_2(C_5H_4MgCl)_2{\cdot}4THF$ with $ZrCl_4$ in toluene gave **8a** in a yield of ca. 40%.

$(C_5H_{10})_2C_2(C_5H_4)_2ZrCl_2$ (8a). Yield: 41%. ^{1}H NMR (600.1 MHz, $CDCl_3$): δ 6.01 (m, 4H, α-Cp), 6.61 (m, 4H, β-Cp), 1.05−2.13 (m, 20H, CH_2). $^{13}C\{^1H\}$ NMR (150.9 MHz, $CDCl_3$): δ 109.81 (4C, α-Cp), 123.55 (4C, β-Cp), 141.89 (2C, ipso-Cp), 23.18 (4C, CH_2), 25.72 (2C, CH_2), 35.85 (4C, CH_2), 50.86 (2C, bridge-C). Anal. Calcd for $C_{22}H_{28}Cl_2Zr$: C, 58.13; H, 6.21. Found: C, 57.51 ; H, 5.64.

Further complexes, $Me_2Si(C_5H_3$-2-Me-4-^{t}Bu-$)_2ZrCl_2$ **(9a)**,[44] Me_2Si(1-indenyl)$_2ZrCl_2$ **(10a)**,[45] C_2H_4(1-indenyl)$_2ZrCl_2$ **(11a)**,[46,47] and Me_2Si(2-Me-benz[e]indenyl)$_2ZrCl_2$ **(12a)**,[48] were likewise prepared as previously described.

The corresponding dibromide compounds **1b,**[49] **2b,**[50] **3b,**[51] **4b, 5b,**[39] **6b, 7b**[52] , and **8b** were obtained by reaction of **1a-8a** with BBr_3, as described by Druce and Lappert,[49] in almost quantitative yields.

$(C_5H_4{}^tBu)ZrBr_2$ (4b). Yield: 85%. ^{1}H NMR (600.1 MHz, $CDCl_3$): δ 6.33 (m, 4H, α-Cp), 6.53 (m, 4H, β-Cp), 1.33 (s, 18H, ^{t}Bu). $^{13}C\{^1H\}$ NMR (150.9 MHz, $CDCl_3$): δ 112.62 (4C, α-Cp), 116.40 (4C, β-Cp), 143.65 (2C, ipso-Cp), 31.50 (6C, ^{t}Bu), 33.65 (2C, ^{t}Bu). Anal. Calcd for $C_{18}H_{26}Br_2Zr$: C, 43.82; H, 5.31. Found: C, 43.29 ; H, 5.20.

$Me_4C_2(C_5H_4)_2ZrBr_2$ (6b). Yield: 91%. ^{1}H NMR (600.1 MHz, $CDCl_3$): δ 6.13 (m, 4H, α-Cp), 6.84 (m, 4H, β-Cp), 1.42 (s, 12H, Me). $^{13}C\{^1H\}$ NMR (150.9 MHz, $CDCl_3$): δ 108.88 (4C, α-Cp), 123.24 (4C, β-Cp), 142.97 (2C, ipso-Cp), 28.34 (4C, Me), 45.27 (2C, bridge-C). Anal. Calcd for $C_{16}H_{20}Br_2Zr$: C, 41.47; H, 4.35. Found: C, 41.58 ; H, 4.45.

$(C_5H_{10})_2C_2(C_5H_4)_2ZrBr_2$ (8b). Yield: 90%. ^{1}H NMR (600.1 MHz, $CDCl_3$): δ 6.10 (m, 4H, α-Cp), 6.89 (m, 4H, β-Cp), 1.14−2.17 (m, 20H, CH_2). $^{13}C\{^1H\}$ NMR (150.9 MHz, $CDCl_3$): δ 110.26 (4C, α-Cp), 124.01 (4C, β-Cp), 141.85 (2C, ipso-Cp), 23.54 (4C, CH_2), 26.08 (2C, CH_2), 35.19 (4C, CH_2), 51.42 (2C, bridge-C). Anal. Calcd for $C_{22}H_{28}Br_2Zr$: C, 48.62; H, 5.19. Found: C, 47.32; H, 4.59.

The dimethyl complexes **1c,**[53] **2c,**[54] **3c,**[55] **4c,**[55] **5c,**[56] **6c,**[57] **7c,**[56] and **8c** were prepared by a method described by Samuel and Rausch:[53] To the zirconocene dichlorides, suspended in diethyl ether at −50° C, a slight excess (2-3%) of 1.6 M methyllithium in diethyl ether solution was added. After being heated slowly

(17) Kutzelnigg, W. *Isr. J. Chem.* **1980**, *19*, 193.
(18) Schindler, M.; Kutzelnigg, W. *J. Chem. Phys.* **1982**, *76*, 1919.
(19) Kutzelnigg, W.; Fleischer, U.; Schindler, M., In *NMR Basic Principles and Progress;* Springer-Verlag: Berlin, 1990; Vol. 23, p 165.
(20) Meier, U.; Wüllen, C. v.; Schindler, M. *J. Comput. Chem.* **1992**, *13*, 551.
(21) Ditchfield, R. *Mol. Phys.* **1974**, *27*, 789.
(22) Wolinski, K.; Hinton, J. F.; Pulay, P. *J. Am. Chem. Soc.* **1990**, *112*, 8251.
(23) Häser, M.; Ahlrichs, R.; Baron, H. P.; Weis, P.; Horn, H. *Theor. Chim. Acta* **1992**, *83*, 455.
(24) Gauss, J. *J. Chem. Phys.* **1993**, *99*, 3629.
(25) Gauss, J.; Stanton, J. F. *J. Chem. Phys.* **1995**, *102*, 251.
(26) Chesnut, D. B.; Rusiloski, B. E.; Moore, K. D.; Egolf, D. A. *J. Comput. Chem.* **1993**, *14*, 1364.
(27) Bühl, M.; Schleyer, P. v. R. *J. Am. Chem. Soc.* **1992**, *114*, 477.
(28) For a recent monograph on methods and applications see e.g.: Tossel, J. A., Ed. *Nuclear Magnetic Shieldings and Molecular Structure*; Kluwer Academics: Amsterdam, 1993.
(29) Loos, D.; Schnöckel, H.; Gauss, J.; Schneider, U. *Angew. Chem., Int. Ed. Engl.* **1992**, *31*, 1362.
(30) Bühl, M.; Thiel, W.; Fleischer, U.; Kutzelnigg, W. *J. Phys. Chem.* **1995**, *99*, 4000.
(31) Bühl, M.; Gauss, J.; Stanton, J. F. *Chem. Phys. Lett.* **1995**, *241*, 248.
(32) Nakatsuji, H. In *Nuclear Magnetic Shieldings and Molecular Structure*; Tossell, J. A., Ed.; Kluwer Academics: Amsterdam, 1993; p 263.
(33) For recent applications of ^{129}Xe chemical shift calculations see: Freitag, A.; Wüllen, C. v.; Staemmler, V. *Chem. Phys.* **1995**, *192*, 267.
(34) Heyn, B., Hipler, B., Kreisel, G., Schreer, H., Walther, D., Eds. *Anorganische Synthesechemie: Ein integriertes Praktikum*; Springer-Verlag: Berlin, 1986.
(35) Wailes, P. C.; Weigold, H.; Bell, A. P. *J. Organomet. Chem.* **1971**, *33*, 181.
(36) Bercaw, J. E.; Marvich, R. H.; Bell, L. G.; Brintzinger, H. H. *J. Am. Chem. Soc.* **1972**, *94*, 1219.
(37) Jordan, R. F.; LaPointe, R. E.; Bradley, P. K.; Baenziger, N. *Organometallics* **1989**, *8*, 2892.
(38) Howie, R. A.; McQuillan, G. P.; Thompson, D. W.; Lock, G. A. *J. Organomet. Chem.* **1986**, *303*, 213.
(39) Antiñolo, A.; Lappert, M. F.; Singh, A.; Winterborn, D. J. W.; Engelhardt, L. M.; Raston, C. L.; White, A. H.; Carty, A. J.; Taylor, N. J. *J. Chem. Soc., Dalton Trans.* **1987**, 1463.
(40) Schwemmlein, H.; Brintzinger, H. H. *J. Organomet. Chem.* **1983**, *254*, 69.
(41) Klouras, N.; Köpf, H. *Monatsh. Chem.* **1981**, *112*, 887.
(42) Bajgur, C. S.; Tikkanen, W. R.; Petersen, J. L. *Inorg. Chem.* **1985**, *24*, 2539.
(43) Burger, P.; Diebold, J.; Gutmann, S.; Hund, H. U.; Brintzinger, H. H. *Organometallics* **1992**, *11*, 1319.
(44) Wiesenfeldt, H.; Reinmuth, A.; Barsties, E.; Evertz, K.; Brintzinger, H. H. *J. Organomet. Chem.* **1989**, *369*, 359.
(45) Herrmann, W. A.; Rohrmann, J.; Herdtweck, E.; Spaleck, W.; Winter, A. *Angew. Chem., Int. Ed. Engl.* **1989**, *28*, 1511.
(46) Wild, F. R. W. P.; Zsolnai, L.; Huttner, G.; Brintzinger, H. H. *J. Organomet. Chem.* **1982**, *232*, 233.
(47) Wild, F. R. W. P.; Wasiucionek, M.; Huttner, G.; Brintzinger, H. H. *J. Organomet. Chem.* **1985**, *288*, 63.
(48) Stehling, U.; Diebold, J.; Kirsten, R.; Röll, W.; Brintzinger, H. H.; Jüngling, S.; Mülhaupt, R.; Langhauser, F. *Organometallics* **1994**, *13*, 964.
(49) Druce, P. M.; Kingston, B. M.; Lappert, M. F.; Spalding, T. R.; Srivastava, R. C. *J. Chem. Soc. A* **1969**, 2106.
(50) Wochner, F.; Brintzinger, H. H. *J. Organomet. Chem.* **1986**, *309*, 65.
(51) Wielstra, Y.; Gambarotta, S.; Meetsma, A.; Spek, A. L. *Organometallics* **1989**, *8*, 2948.
(52) Köpf, H.; Klouras, N. *Z. Naturforsch.* **1983**, *38b*, 321.
(53) Samuel, E.; Rausch, M. D. *J. Am. Chem. Soc.* **1973**, *95*, 6263.
(54) Manriquez, J. M.; McAlister, D. R.; Rosenberg, E.; Shiller, A. M.; Williamson, K. L.; Chan, S. I.; Bercaw, J. E. *J. Am. Chem. Soc.* **1978**, *100*, 3078.
(55) Couturier, S.; Tainturier, G.; Gautheron, B. *J. Organomet. Chem.* **1980**, *195*, 291.
(56) Siedle, A. R.; Newmark, R. A.; Lamanna, W. M.; Schroepfer, J. N. *Polyhedron* **1990**, *9*, 301.
(57) Niemann, U.; Diebold, J.; Troll, C.; Rief, U.; Brintzinger, H. H. *J. Organomet. Chem.* **1993**, *456*, 195.

to room temperature, the solutions were stirred for an additional 1 h. Solvents were removed in vacuo, and the residue was extracted with pentane. Crystallization at −78 °C afforded the complexes as colorless crystals in yields of 60-90%.

$(C_5H_{10})_2C_2(C_5H_4)_2ZrMe_2$ (8c). Yield: 57%. ^{1}H NMR (600.1 MHz, $CDCl_3$): δ 5.52 (m, 4H, α-Cp), 6.46 (m, 4H, β-Cp), 0.95−1.65 (m, 20H, CH_2), 0.03 (s, 6H, CH_3). $^{13}C\{^1H\}$ NMR (150.9 MHz, $CDCl_3$): δ 107.74 (4C, α-Cp), 115.34 (4C, β-Cp), 131.93 (2C, ipso-Cp), 23.60 (4C, CH_2), 26.29 (2C, CH_2), 34.66 (4C, CH_2), 49.53 (2C, bridge-C), 27.96 (2C, CH_3).

2. NMR Measurements. The ^{91}Zr NMR spectra were recorded on a Bruker AMX-600 spectrometer at 55.76 MHz with a standard broad-band probe at 300 ± 1 K or 348 ± 1 K, using a pulse width of 18 μs (ca. 90°) and a repetition delay of 150 ms. The number of scans were ca. 150 for narrow and 50 000 for broad signals, and the aquisition time was ≤0.05 s. The ^{91}Zr chemical-shift values, $\delta(^{91}Zr)$, are reported relative to a saturated solution of $(C_5H_5)_2ZrBr_2$ as an external reference. The FID was treated with a line-broadening function. The line widths at half-height ($\Delta\nu_{1/2}$) of the ^{91}Zr signals are reported in Hz. The $T_1(^{13}C)$ values were obtained from 0.1 M degassed samples by the standard inversion-recovery method with a triple resonance (^{1}H, ^{13}C, ^{15}N) 5 mm probe on the same instrument. The spectra were recorded with a recycle time of ca. $10T_1$.

Sample Preparation. All manipulations were performed under argon by the use of Schlenk techniques or in a nitrogen-filled vacuum glovebox. NMR tubes and other glassware in contact with zirconocene solutions were previously dried by heating under a vacuum. Solvents were dried and destilled over sodium/benzophenone or calcium hydride under argon atmosphere. NMR solvents (*d*-chloroform, d_6-benzene, d_8-toluene, d_8-tetrahydrofuran) were dried in the same manner, desoxygenated, and stored over molecular sieves (4 Å) in a nitrogen atmosphere. Solutions of the zirconocene complexes were prepared as concentrated as possible, transferred into 5 mm OD NMR tubes, degassed, and sealed in vacuo. The samples for the high-temperature NMR measurements were sealed under atmospheric pressure of argon.

3. Structural Data. Crystal structures have been reported for zirconocene dichloro complexes **1a**,[58] **3a**,[59] **4a**,[38] **5a**,[39] **7a**,[42] **9a**,[44] and **1c**.[60] The corresponding data for the permethyl complex **2a** have been approximated by those of the closely related complex $(C_5Me_4Et)_2ZrCl_2$.[61] Structural data for the dibromo complex **1b** are based on a crystal structure determination.

Crystal Data for Cp_2ZrBr_2 (1b). $C_{10}H_{10}Br_2Zr$: M = 381.2, a = 7.984(5) Å, b = 12.135(8) Å, c = 12.527(9) Å, α = 71.75(5), β = 79.34(5), γ = 89.36(5)°, V = 1131.4(12) Å^3, triclinic, space group $P\bar{1}$, Z = 4, D_c = 2.238 g/cm^3, radiation Mo Kα (λ = 0.710 73 Å), μ = 7.910 mm^{-1}, $F(000)$ = 720, T = 243 K, crystal size (mm) 0.3 × 0.3 × 0.3, diffractometer Siemens R3m/V. Structure solution and refinement were with Siemens SHELXTL PLUS (VMS) software. Solution: Patterson method. Absorption correction: semiempirical; min/max transmission 0.1199/0.1659. The cell contains two independent molecules. The Cp ring of one molecule is disordered. All non-hydrogen atoms were refined anisotropically, except for the disordered carbon atoms. All hydrogen atom positions were calculated and refined using the riding model technique with fixed isotropic U. Final R = 0.0605, wR = 0.0732, and S = 2.21. Further structural details are in the Supporting Information.

Crystal Data for $Me_4C_2(C_5H_4)_2ZrCl_2$ (6a). Complex **6a** cocrystallizes with one solvent molecule from $CHCl_3$ as a $Me_4C_2(C_5H_4)_2ZrCl_2{\cdot}CHCl_3$ adduct. $C_{17}H_{21}Cl_5Zr$: M = 493.8, a = 10.441(2) Å, b = 8.224(2) Å, c = 23.143(4) Å, β = 96.68-(8)°, V = 1973.6(8) Å^3, monoclinic, space group $P2_1/c$, Z = 4, D_c = 1.662 g/cm^3, radiation Mo Kα (λ = 0.710 73 Å), μ = 1.228 mm^{-1}, $F(000)$ = 992, T = 238 K, crystal size (mm) 0.3 × 0.3 × 0.5, diffractometer Siemens R3m/V. Structure solution and refinement were with Siemens SHELXTL PLUS (VMS) software. Solution was by direct methods. All non-hydrogen atoms were refined anisotropically, and all hydrogen atom positions were calculated and refined using the riding model technique with fixed isotopic U. Final R = 0.0369, wR = 0.0589, and S = 2.32. Further structural details are in the Supporting Information.

4. Ab Initio Calculations of Electric Field Gradients and ^{91}Zr NMR Shifts. The principal values q_{ii} of the EFG tensors have been computed at the SCF level employing the Gaussian 92 program[62] and the following basis sets. Basis A: Zr (17s13p9d)[63,64] contracted to [12s9p5d], including two sets of diffuse p functions[65] (α_p = 0.11323 and 0.04108) and one diffuse d-set (α_d = 0.0382); Br relativistic ME-fit effective core potential (ecp),[66−68] valence [2s2p1d] basis;[69] Cl, Si 3−21G(*);[70] C, H 3−21G.[70] Basis B: Zr same as basis A, decontracted to [12s10p6d] and augmented with additional sets of diffuse p and d functions (exponents chosen as one-third of those of the most diffuse functions of basis A); Br same as basis A, all others 6-31G*.[70] The EFG values are given in atomic units (1 au = 9.717 365 × 10^{21} V m^{-2}) and are ordered so that $|q_{zz}| > |q_{yy}| > |q_{xx}|$. In addition, EFG tensors have been computed employing density functional theory (DFT) using the Becke 1988[71] and the Perdew 1986[72,73] gradient-corrected exchange-correlation functionals together with basis B (denoted as BP86/B).

Geometries have been either taken from X-ray structural analyses (with C−H bond lengths set to 1.09 Å) or have been fully optimized[70] in the given symmetry at the SCF level employing basis B′, i.e. same as basis B but using a relativistic ME-fit ecp and a valence [5s5p2d] basis on Zr.[74]

NMR chemical shifts have been computed using SCF/B′ geometries, IGLO-SCF,[17−19] or GIAO-SCF[21,22] methods in their direct versions,[20,23] as implemented in the TURBOMOLE program[75] and the following basis sets. II: Zr same as A, IGLO-basis II[19] for the rest, i.e. Br (15s11p7d2f)/[10s9p5d2f]; Cl (11s7p2d)/[7s6p2d]; C (9s5p1d)/[5s4p1d]; H (5s1p)/[3s1p]. III′: Zr same as A, decontracted to (13s11p8d); Br same as II, decontracted to [11s10p6d2f]; Cl (12s8p3d)/[8s7p3d]; C,H same as basis II. Zr chemical shifts are reported relative to $(C_5H_5)_2ZrBr_2$, the experimental standard (C_2 symmetry, SCF/B′ geometry), with absolute, computed shieldings σ[76] of 2917.5 (IGLO-SCF/II),[77] 2359.5 (IGLO-SCF/III′), 2518.1 (GIAO-SCF/II), and 2477.7 ppm (GIAO-SCF/III′).

(58) Soloveichik, G. L.; Arkhireeva, T. M.; Bel'skii, V. K.; Bulychev, B. M. *Metalloorg. Khim.* **1988**, *1*, 226.
(59) Petersen, J. L.; Egan, J. W. *Inorg. Chem.* **1983**, *22*, 3571.
(60) Hunter, W. E.; Hrncir, D. C.; Bynum, R. V.; Penttila, R. A.; Atwood, J. L. *Organometallics* **1983**, *2*, 750.
(61) Kurz, S.; Hey-Hawkins, E. *Z. Krist.* **1993**, *205*, 61.
(62) Frisch, M. J.; Trucks, G. W.; Schlegel, H. B.; Gill, P. M. W.; Johnson, B. G.; Wong, M. W.; Foresman, J. B.; Robb, M. A.; Head-Gordon, M.; Replogle, E. S.; Gomperts, R.; Andres, L.; Raghavachari, K.; Binkley, J. S.; Gonzales, C.; Martin, R. L.; Fox, D. J.; DeFrees, D. J.; Baker, J.; Stewart, J. J. P.; Pople, J. A., Gaussian92/DFT: Pittsburgh, PA, 1993.
(63) Horn, H. unpublished data.
(64) Schäfer, A.; Horn, H.; Ahlrichs, R. *J. Chem. Phys.* **1992**, *97*, 2571.
(65) Walch, S. P.; Bauschlicher, C. W.; Nelin, C. J. *J. Chem. Phys.* **1983**, *79*, 3600.
(66) Dolg, M.; Wedig, U.; Stoll, H.; Preuss, H. *J. Chem. Phys.* **1987**, *86*, 866.
(67) Dolg, M. Ph.D. Thesis, University of Stuttgart, 1989.
(68) Schwerdtfeger, P.; Dolg, M.; Schwarz, W. H. E.; Bowmaker, G. A.; Boyd, P. D. W. *J. Chem. Phys.* **1989**, *91*, 1762.
(69) Kaupp, M.; Schleyer, P. v. R.; Stoll, H.; Preuss, H. *J. Am. Chem. Soc.* **1991**, *113*, 6012.
(70) Hehre, W. J.; Radom, L.; Schleyer, P. v. R.; Pople, J. A. *Ab initio Molecular Orbital Theory*; Wiley: New York, 1986.
(71) Becke, A. D. *Phys. Rev. A* **1988**, *38*, 3098.
(72) Perdew, J. P. *Phys. Rev. B* **1986**, *33*, 8822.
(73) Perdew, J. P. *Phys. Rev. B* **1986**, *34*, 7406.
(74) Andrae, D.; Häussermann, U.; Dolg, M.; Stoll, H.; Preuss, H. *Theor. Chim. Acta* **1990**, *77*, 123.
(75) Ahlrichs, R.; Bär, M.; Häser, M.; Horn, H.; Kölmel, C. *Chem. Phys. Lett.* **1989**, *162*, 165.

Chart 1

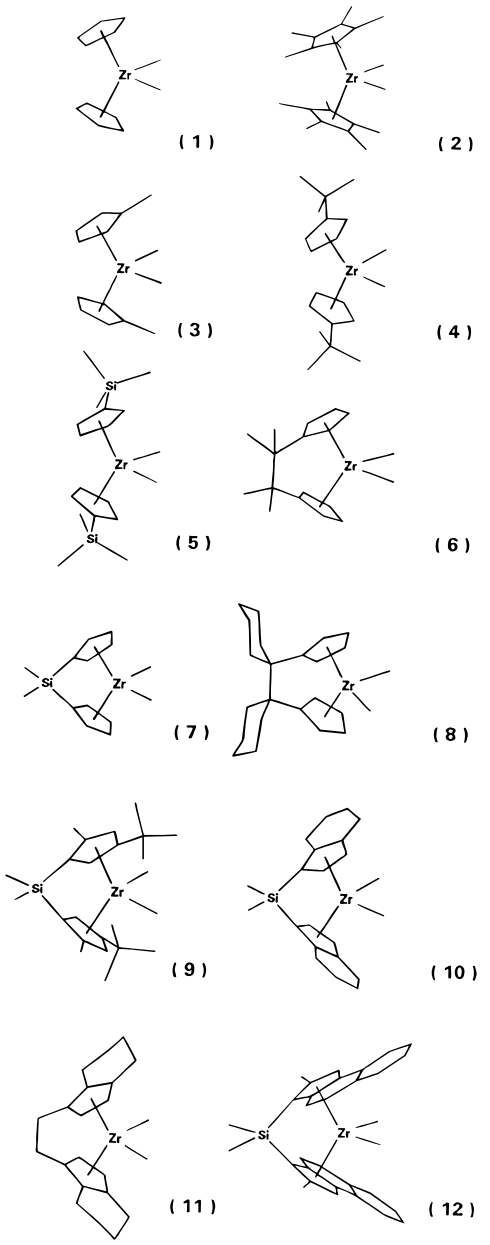

Results and Discussion

1. ^{91}Zr NMR Spectra. The experimental chemical shift data for the investigated Zr complexes (Chart 1) are compiled in Table 1.

^{91}Zr NMR signals have been observed for complexes **1a**−**8a**, **1b**−**8b**, and **1c**−**7c**. For complexes **8c, 9a**−**12a**, and **10b**−**12b,** ^{91}Zr NMR signals could not be detected even at 353 K; for these complexes we estimate line widths $\Delta\nu_{1/2} > 10$ KHz. The ^{91}Zr chemical shift range is quite large (−112 to 893 ppm) and can be divided into four regions: −112 to −32 ppm for the zirconocene dichloride complexes **1a**−**8a**, [with the exception of $(C_5Me_5)_2ZrCl_2$ **(2a)**, 85 ppm], 0 to 80 ppm for zirconocene dibromide complexes **1b-8b** [with the exception of $(C_5Me_5)_2ZrBr_2$ **(2b)**, 240 ppm], 386 to 451 ppm for zirconocene dimethyl complexes, and finally 628 ppm for $ZrCl_4$·2THF **(13)** and 893 ppm for $Zr(NMe_2)_4$ **(14)**. The $(C_5H_5)_2ZrX_2$ species (X= halogen) exhibit an inverse halogen effect probably due to the dominance of the paramagnetic term in the chemical shift tensor.[12,15] The strong deshielding of the permethylated complexes **3a** and **3b** was found by Benn and explained by a lowering of the mean excitation energies.[15]

There is only a very small concentration effect observable on the ^{91}Zr chemical shift for a series of $(C_5Me_5)_2ZrCl_2$ **(2a)** samples with concentrations ranging from 0.03 to 0.25 M in $CDCl_3$, the variation $\Delta\delta(^{91}Zr)$ being only ±0.1 ppm. Likewise, the temperature has a small effect on the chemical shift of **2a**: 85.5 ppm (295 K) and 86.3 ppm (330 K). More pronounced temperature effects are observed for **2c**−**7c**. As is common for other quadrupolar nuclei, the line widths are considerably more sensitive to temperature changes: for **2a,** $\Delta\nu_{1/2}$ decreases from 59 Hz at 295 K to 50 Hz at 330 K. Even larger effects can be observed for the broad lines of the zirconocene dimethyl complexes. The line width $\Delta\nu_{1/2}$ of $(C_5H_4{}^tBu)_2ZrMe_2$ **(4c)** decreases from 8250 to 3230 Hz upon increasing the temperature from 300 to 348 K.

Table 1. ^{91}Zr Chemical Shifts and Line Widths of Zirconocene Complexes[a]

zirconocene complex	solvent	T/K	δ/ppm[89]	$\Delta\nu_{1/2}$/Hz
Cp_2ZrCl_2 **(1a)**[4]	$CDCl_3$	300	−112	270
Cp_2ZrBr_2 **(1b)**[4]	$CDCl_3$	300	0	16
Cp_2ZrBr_2 **(1b)**[4]	C_6D_6	300	0	18
$Cp_2Zr(Cl)Me$ **(1d)**[6]	$CDCl_3$	300	126	1480
Cp_2ZrMe_2 **(1c)**[6]	C_6D_6	300	386	2530
Cp_2ZrMe_2 **(1c)**	C_6D_6	348	387	1070
$(C_5Me_5)_2ZrCl_2$ **(2a)**[5]	$CDCl_3$	300	85	57
$(C_5Me_5)_2ZrBr_2$ **(2b)**	$CDCl_3$	300	240	450
$(C_5Me_5)_2ZrMe_2$ **(2c)**	C_6D_6	300	443	3910
$(C_5Me_5)_2ZrMe_2$ **(2c)**	C_6D_6	348	451	2240
$(C_5H_4Me)_2ZrCl_2$ **(3a)**[7]	$CDCl_3$	300	−69	540
$(C_5H_4Me)_2ZrBr_2$ **(3b)**	$CDCl_3$	300	56	140
$(C_5H_4Me)_2ZrMe_2$ **(3c)**	C_6D_6	300	401	4030
$(C_5H_4Me)_2ZrMe_2$ **(3c)**	C_6D_6	348	406	1630
$(C_5H_4{}^tBu)_2ZrCl_2$ **(4a)**[7]	$CDCl_3$	300	−61	2810
$(C_5H_4{}^tBu)_2ZrCl_2$ **(4a)**	d_8-Tol	348	−64	1130
$(C_5H_4{}^tBu)_2ZrBr_2$ **(4b)**	$CDCl_3$	300	61	1700
$(C_5H_4{}^tBu)_2ZrMe_2$ **(4c)**	C_6D_6	300	438	8250
$(C_5H_4{}^tBu)_2ZrMe_2$ **(4c)**	C_6D_6	348	422	3230
$(C_5H_4SiMe_3)_2ZrCl_2$ **(5a)**[56]	C_6D_6	300	−89	1250
$(C_5H_4SiMe_3)_2ZrBr_2$ **(5b)**	C_6D_6	300	28	260
$(C_5H_4SiMe_3)_2ZrMe_2$ **(5c)**[56]	d_8-Tol	348	410	3240
$Me_4C_2(C_5H_4)_2ZrCl_2$ **(6a)**	$CDCl_3$	300	−48	700
$Me_4C_2(C_5H_4)_2ZrBr_2$ **(6b)**	$CDCl_3$	300	65	83
$Me_4C_2(C_5H_4)_2ZrMe_2$ **(6c)**	C_6D_6	300	432	5310
$Me_4C_2(C_5H_4)_2ZrMe_2$ **(6c)**	C_6D_6	348	429	2160
$Me_2Si(C_5H_4)_2ZrCl_2$ **(7a)**	$CDCl_3$	300	−95	1820
$Me_2Si(C_5H_4)_2ZrBr_2$ **(7b)**	C_6D_6	300	13	360
$Me_2Si(C_5H_4)_2ZrMe_2$ **(7c)**[56]	d_8-Tol	300	427	4520
$Me_2Si(C_5H_4)_2ZrMe_2$ **(7c)**	d_8-Tol	348	419	2500
$(C_5H_{10})C_2(C_5H_4)_2ZrCl_2$ **(8a)**	$CDCl_3$	300	−32	1000
$(C_5H_{10})C_2(C_5H_4)_2ZrBr_2$ **(8b)**	$CDCl_3$	300	80	490
$ZrCl_4$·2THF **(13)**	d_8-THF	300	628	2920
$Zr(NMe_2)_4$ **(14)**	C_6D_6	300	893	1130

[a] No signals were detectable for the following complexes: $(C_5H_{10})C_2(C_5H_4)_2ZrMe_2$ **(8c)**, *rac*-$Me_2Si(C_5H_2$-2-Me-4-$^tBu)_2ZrCl_2$ **(9a)**, *rac*-Me_2Si-(1-ind)$_2ZrCl_2$ **(10a)**, *rac*-$Me_2Si(ind)_2ZrBr_2$ **(10b)**, *rac*-C_2H_4(1-ind)$_2ZrCl_2$ **(11a)**, *rac*-Me_2Si(2-Me-benz[*e*]-indenyl)$_2ZrCl_2$ **(12a)**, and *rac*-Me_2Si(2-Me-benz[*e*]indenyl)$_2ZrBr_2$ **(12b)**.

(76) The σ value denotes shielding relative to the bare nucleus and is converted to δ values according to $\delta = \sigma$(standard) − σ. Note the different sign convention for σ, larger values denote increasing shielding.

(77) By default, core and valence orbitals are localized separately, with the Zr 4s and 4p orbitals included in the former. If these orbitals are localized together with the valence shell, somewhat different absolute shieldings are obtained; the relative δ values, however, are affected only by a few ppm.

Table 2. Ab Initio Computed Electric Field Gradients q_{ii}[a] for Zirconocenes

compd	level	q_{zz}	q_{yy}	q_{xx}	η[b]
Cp_2ZrBr_2 **(1b)**	SCF/A	−0.2470	0.2336	0.0134	0.891
	SCF/B	−0.2043	0.1776	0.0267	0.739
	BP86/B	−0.2056	0.1575	0.0481	0.532
Cp_2ZrCl_2 **(1a)**	SCF/A	−0.3345	0.2451	0.0895	0.465
	SCF/B	−0.2903	0.2498	0.0404	0.721
	BP86/B	−0.2375	0.1839	0.0536	0.549
Cp_2ZrMe_2 **(1c)**	SCF/A	−0.9950	0.6399	0.3551	0.286
	SCF/B	−0.8859	0.5880	0.2979	0.327
	BP86/B	−0.7965	0.5966	0.1999	0.498

[a] Eigenvalues of the diagonalized efg tensor in atomic units, ordering $|q_{zz}| > |q_{yy}| > |q_{xx}|$; X-ray-derived geometries employed.[58,60] [b] Asymmetry parameter η; for definition see text.

As quadrupolar relaxation governs the line width of the ^{91}Zr resonance, the greatly varying line widths of the investigated zirconocene complexes are related to the respective molecular structures *via* changes of the electric field gradient components, q_{ii}, and of the isotropic molecular correlation times τ_c.

$$\Delta\nu_{1/2} \propto {q_{zz}}^2\left(1 + \frac{\eta^2}{3}\right)\tau_c \qquad (1)$$

In this product, q_{zz} is the largest component of the electric field gradient (EFG) and η is the asymmetry parameter defined as $(q_{xx} - q_{yy})/q_{zz}$. Apart from temperature and viscosity, τ_c depends primarily on the molecular size and should increase with the latter. If all other parameters were equal, $(C_5H_5)_2ZrBr_2$ **(1b)** should, therefore, yield a broader ^{91}Zr resonance than $(C_5H_5)_2ZrCl_2$ **(1a)**, and $\Delta\nu_{1/2}$ for $(C_5H_5)_2ZrMe_2$ **(1c)** should be of the same order of magnitude. However, the $\Delta\nu_{1/2}$ values recorded for the $(C_5H_5)_2ZrX_2$ species are 18, 270, and 2530 Hz for X = Br, Cl, and Me, respectively, showing a different sequence and an unexpectedly large variation. It has thus been suspected that variations in q_{zz} and/or η are dominant in these cases.

2. EFG Calculations. EFGs and asymmetry parameters η for $(C_5H_5)_2ZrX_2$ (X = Br, Cl, Me), computed at various ab initio levels and employing X-ray-derived geometries are collected in Table 2. The absolute q_{ii} values ($i = x, y, z$) depend strongly on the basis set and on the theoretical level that is used. In general, enlargement of the basis set decreases the computed q_{ii} values considerably (compare SCF/A and SCF/B values in Table 2). Inclusion of electron correlation also affects q_{ii}, mostly resulting in further, smaller reductions (compare SCF/B and BP86/B data). Thus, quantitative calculations of EFGs appear very difficult for these molecules. This also holds, more pronounced, for the asymmetry parameter η which can even oscillate strongly with the theoretical level (see Table 2). Since small numbers and differences between these govern the magnitude of η in zirconocenes, even qualitative estimates of η based on ab initio data seem virtually impossible at this time.

According to eq 1, however, η affects $\Delta\nu_{1/2}$ via the factor $(1 + (\eta^2/3))$. Since η assumes values between 0 and 1, this factor can only vary between 1 and 1.33, and the other parameters in eq 1, q_{zz} in particular, may be more important. In fact, the absolute numbers of q_{zz} computed for $(C_5H_5)_2ZrMe_2$ **(1c)** are ca. three times as large as those obtained for $(C_5H_5)_2ZrCl_2$ **(1a)** (Table 2), *irrespective of the theoretical level* (the ratios are ca. 2.97, 3.05, and 3.35 at SCF/A, SCF/B, and BP86/B levels, respectively)! Likewise, the computed q_{zz} ratios between **1a** and Cp_2ZrBr_2 **(1b)** are rather similar for the various methods (ca. 1.35, 1.42, and 1.16 at SCF/A, SCF/B, and BP86/B, respectively). The computed $|q_{zz}|$ values for $(C_5H_5)_2ZrX_2$ increase with the experimental line widths, i.e. in the sequence Br < Cl < Me. It thus appears that, unlike the absolute, quantitative numbers, the relative trends in q_{zz} from one molecule to the other can be described with ab initio levels, at least qualitatively.

Subsequently, EFGs of several other zirconocenes have been computed at a moderate theoretical level, SCF/B, employing the solid-state structures. The results are summarized and related to the experimental line widths in Table 3. The trends can be best compared by looking at the $\Delta\nu_{1/2}$(rel) and ${q_{zz}}^2$(rel) values, i.e. the ratios with respect to the corresponding data for $(C_5H_5)_2ZrCl_2$ (last two columns in Table 3). In the series $(C_5H_5)_2ZrX_2$ (X = Br, Cl, Me), the $\Delta\nu_{1/2}$(rel) and ${q_{zz}}^2$(rel) values are very similar, covering almost 2 orders of magnitude. It thus appears that for these molecules, the variation of $\Delta\nu_{1/2}$ is mainly governed by the changes in q_{zz}. For the substituted species $(C_5H_4R)_2ZrCl_2$ (R = H, Me, ^{t}Bu) **(3a−c, 4a−c)**, however, the changes in ${q_{zz}}^2$(rel) are much smaller than the variations in $\Delta\nu_{1/2}$(rel). These data, therefore, suggest that the electronic influence of the alkyl groups R is rather small and that the broadening of the signals for R = Me and ^{t}Bu is mainly caused by larger correlation times τ_c due to the increasing bulkiness of the ligands.

3. Correlation Times τ_c. Additional support for this interpretation comes from isotropic τ_c values obtained from T_1 relaxation times and NOE values of the ^{13}C nuclei of the cyclopentadienyl ligands. The ^{13}C relaxation time $T_{1dd}(^{13}C)$ due to C−H dipolar interaction is approximated by[78]

$$\frac{1}{T_{1dd}(^{13}C)} = \frac{{\mu_0}^2 N\gamma(^1H)^2\gamma(^{13}C)^2\hbar^2\tau_c}{16\pi^2 {r_{CH}}^6} = NK\tau_c \qquad (2)$$

$$K = 2.147 \times 10^{10}\ s^{-2} \qquad \text{(cf. ref. 79)}$$

where τ_c is the isotropic correlation time. Dipolar interactions from nonbonded protons can be neglected because of the much larger distances with respect to the C−H bond lengths (cf. the $1/r^6$ dependence in eq 2), and only N, the number of directly attached protons to the carbon, is of interest. The C−H distances are assumed as constant (1.09 Å). According to eq 2, τ_c can be calculated from the dipole−dipole relaxation time $T_{1dd}(^{13}C)$, the interatomic distance r_{CH}, the number of directly attached protons N, and the magnetogyric ratio $\gamma(^1H)$ and $\gamma(^{13}C)$. $T_{1dd}(^{13}C)$ can directly be obtained from the NOE factor and the relaxation time $T_1(^{13}C)$ (eq 3).

$$\mathrm{NOE} = 1 + \frac{2T_1(^{13}C)}{T_{1dd}(^{13}C)} \qquad (3)$$

$T_1(^{13}C)$ values of the zirconocene compounds **1a, 2a, 3a, 4a, 5a,** and **7a** have been determined with the standard inversion-recovery NMR experiment. The NOE values

(78) Abragam, A., Ed. *The Principles of Nuclear Magnetism*; Oxford University Press: Oxford, U.K., 1961; Chapter 9.

(79) $\mu_o = 4\pi \times 10^{-7}$ m kg s^{-2} A^{-2}; $\gamma(^1H) = 2.6752 \times 10^8$ kg^{-1} s A rad; $\gamma(^{13}C) = 0.6726 \times 10^8$ kg^{-1} s A rad; $r_{CH} = 1.09$ Å.

Table 3. Relation between Experimental ^{91}Zr NMR Line Widths $\Delta\nu_{1/2}$, Computed EFGs,[a] and Tilt Angles τ for Zirconocenes

compd	$\Delta\nu_{1/2}$/Hz	q_{zz}	$\Delta\nu_{1/2}$(rel)[b]	q_{zz}^2(rel)[b]	τ/deg
Cp_2ZrBr_2 **(1b)**	16	-0.2043	0.1	0.5	
Cp_2ZrCl_2 **(1a)**	270	-0.2903	1.0	1.0	
Cp_2ZrMe_2 **(1c)**	2530	-0.8859	9.4	9.3	
$(C_5Me_5)_2ZrCl_2$ **(2a)**	57	-0.1772	0.2	0.3	0.8
Cp_2ZrCl_2 **(1a)**	270	-0.2903	1.0	1.0	0.7
$(C_5H_4Me)_2ZrCl_2$ **(3a)**	540	-0.2453	2.0	0.7	1.7
$(C_5H_4{}^tBu)_2ZrCl_2$**(4a)**	2810	-0.4074	10.4	2.0	2.9
$(C_5H_4SiMe_3)_2ZrCl_2$ **(5a)**	1250	-0.1496	4.6	0.3	0.8
rac-$Me_2Si(C_5H_4)_2ZrCl_2$ **(7a)**	1820	-0.4830	6.7	2.8	2.8
rac-$Me_2Si(C_5H_2$-2-Me- 4-$^tBu)_2ZrCl_2$ **(9a)**[c]	n.d.[d]	-0.7062		5.9	4.5

[a] Largest components, q_{zz}, computed at the SCF/B level employing X-ray-derived geometries. [b] Ratio with respect to the value for Cp_2ZrCl_2. [c] In the calculation, the solid-state structure has been employed with t-Bu and Me substituents replaced by H. [d] Not detected.

Table 4. Relaxation Times T_1(^{13}C), NOE, and Correlation Times τ_c of Zirconocene Dichloride Complexes

compd	T_1/s	NOE	T_{1DD}/s	$10^{-12}\tau_c$/s	τ_c(rel)
$(C_5H_5)_2ZrCl_2$ **(1a)**	8.60 (CH)	2.30	13.2	3.5	1.0
$(C_5H_4Me)_2ZrCl_2$ **(3a)**	5.60 (CH)	2.28	8.8	5.3	
	5.71 (CH)	2.55	7.4	6.3	1.8
$(C_5H_4{}^tBu)_2ZrCl_2$**(4a)**	2.41 (CH)	2.34	4.2	11.0	
	2.39 (CH)	2.79	5.4	17.1	4.9
$(C_5H_4SiMe_3)_2ZrCl_2$ **(5a)**	2.00 (CH)	2.67	2.4	19.4	
	1.95 (CH)	2.65	2.4	19.7	5.6
$Me_2Si(C_5H_4)_2ZrCl_2$ **(7a)**	2.83 (CH)	2.36	4.2	11.2	3.2
	3.41 (CH)	2.27	5.4	8.7	

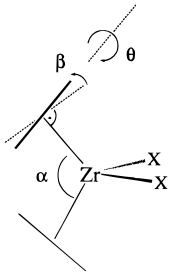

Figure 1. Schematic representation of zirconocenes Cp_2ZrX_2 indicating geometrical parameters.

of the ^{13}C atoms have been obtained from comparisons of the intensities of the ^{13}C resonances of inverse gated and continously composite pulse ^{1}H-decoupled ^{13}C NMR spectra (Table 4).

The relative correlation times τ_c(rel) for $(C_5H_5)_2ZrCl_2$ **(1a)**, $(C_5H_4Me)_2ZrCl_2$ **(3a),** $(C_5H_4{}^tBu)_2ZrCl_2$ **(4a)**, $(C_5H_4SiMe_3)_2ZrCl_2$ **(5a)**, and $Me_2Si(C_5H_4)_2ZrCl_2$ **(7a)** confirm our suggestion that τ_c is the dominant factor for the relative line widths in these cases. Even though larger in size than the parent $(C_5H_5)_2ZrCl_2$ **(1a)**, $(C_5Me_5)_2ZrCl_2$ **(2a)** shows a narrower line in the ^{91}Zr NMR spectrum. According to the data in Table 3, the smaller $\Delta\nu_{1/2}$ of **2a** is largely due to the decrease of q_{zz}.

4. Coordination Geometries. *ansa*-compounds bearing a dimethylsilylene bridge between the two Cp rings show broad ^{91}Zr NMR resonances. *ansa*-$Me_2Si(C_5H_4)_2ZrCl_2$ **(7a)** gives a somewhat increased, computed q_{zz}^2(rel) value (see Table 3), possibly contributing to this line broadening. The signal of a highly substituted derivative, *ansa*-$Me_2Si(C_5H_2$-2-Me-4-$^tBu)_2ZrCl_2$ **(9a)**, is undetectably broad at room temperature. Compound **9a** is rather large for ab initio computations; a calculation has been performed by employing the X-ray structure of **9a** with Me and ^{t}Bu groups replaced by H, i.e. for a "distorted" **7a** geometry. Interestingly, this "distortion" induced by the bulky groups increases the computed relative q_{zz}^2 significantly (ca. by a factor of 2; cf. the last two entries in Table 3). Taking into account the additional line broadening due to the bulky substituents (cf. the factor of ca. 10 in going from **1a** to the ^{t}Bu derivative **4a**), $\Delta\nu_{1/2}$ estimated for **9a** would be much larger than 10.000 Hz, i.e. too broad to be observable. It is unfortunate that the excessive line widths of the catalytically most interesting complexes **9a**−**12a** preclude any correlations between ^{91}Zr NMR data and catalytic properties.

The notable variation of the q_{zz} values computed for the same *ansa*-compounds in two different geometries suggests that geometry effects may be important for the EFGs in zirconocenes. To study the influence of certain geometrical parameters in more detail, EFGs have been computed at the SCF/B level for specifically altered $(C_5H_5)_2ZrCl_2$ geometries. Starting from the solid-state structure, the orientations of the Cp ligands have been varied by separately changing the CpZrCp′ angle, α, the inclination angle, β, or the twist angle, θ (cf. the schematic representation in Figure 1), leaving all other parameters unchanged.

Closing α by 15° increases $|q_{zz}|$ (0.4197), while increasing α by the same amount results in a smaller EFG (0.1289). Larger variations in $|q_{zz}|$ are found upon changes in β by +7.5° (0.7915) and by −7.5° (0.6281) or upon twisting the Cp rings in opposite directions by θ = 7.5° (0.7915). This indicates that the EFG is more dependent on the magnitude of the deviation of the normal to the Cp planes from the direction of the zirconium−zentroid vector, i.e. the tilt angle τ, than on the direction of this distortion. Experimental tilt angles τ are available for a series of zirconocenes **1a**−**5a** and **7a**,and **9a** from X-ray crystallographic analyses[38,39,42,44,58,59] (for **2a** we use the tilt angle determined from the crystal structure of $(C_5Me_4Et)_2ZrCl_2$[61]), and they are listed in Table 3. The experimental ^{91}Zr NMR line widths $\Delta\nu_{1/2}$, the computed q_{zz}^2 (rel) values, and the tilt angle τ exhibit parallel trends. It appears that the exact position of the Zr atom with respect to each Cp ring plane is more important for the EFG than is the CpZrCp′ angle (see also the chemical shift section).

To separate possible inductive effects from these geometrical effects, model calculations have been performed for the zirconocenes **2a**−**7a** with the substituents at the Cp rings replaced by hydrogens, leaving all other parameters unchanged. This procedure affords the parent **1a** but in the geometry of the various, substituted derivatives. In most cases, only minor changes are found for the computed q_{zz} values: e.g., going from R = ^{t}Bu to R = H in $(C_5H_4R)_2ZrCl_2$ **(4a)**

changes q_{zz} from −0.4074 (Table 3) to −0.4718;[80] i.e. the "electronic effect" of the ^{t}Bu group is small. This holds for most other Cp-substituted derivatives, except for $(C_5Me_5)ZrCl_2$ **(2a)**: replacing all methyl groups by hydrogens affords a change in q_{zz} from −0.1772 (Table 3) to −0.3227, close to the value of **1a** (−0.2903). In this case, it appears to be the electronic effect exerted by the highly basic C_5Me_5 ligand that is responsible for the reduction of $|q_{zz}|$ and, hence, of $\Delta\nu_{1/2}$.

Because of the relevance to homogeneous catalysis, structures and reactivities of zirconocenes have recently been studied in great detail, both at the SCF and DFT levels.[81−83] A detailed discussion of the ab initio geometries would be beyond the scope of this paper. Geometry optimizations at the SCF/B′ level of $(C_5H_5)_2ZrX_2$ (X = Br, Cl, Me) afford Zr−X and average Zr−C distances that are somewhat overestimated, e.g. by ca 2 and 8 pm, respectively, for X = Cl with respect to the gas-phase structure.[84] The relative conformations of the two Cp rings are correctly reproduced at that level, i.e. "staggered" for X = Br and Cl (C_2 more stable than C_{2v} by 0.2 kcal/mol each) and "eclipsed" for $(C_5H_5)_2ZrMe_2$ **(1c)** (C_{2v} more stable than C_s by 0.4 kcal/mol).

When the ab initio geometries are employed for the EFG calculations, the results depend somewhat on the relative Cp conformations. When the lowest-energy structures are used, the computed EFGs differ slightly from those in Table 2, obtained for the solid-state geometries, but the trends remain the same. In particular, the q_{zz}^2(rel) values are in good accord for both sets of structures; cf. 0.3, 1, and 9.7 for X = Br, Cl, and Me, respectively (SCF/B′ geometries) vs 0.5, 1, and 9.3, respectively (X-ray-derived geometries, Table 3).

5. ^{91}Zr Chemical Shifts. In order to test how well ^{91}Zr chemical shifts of zirconocenes can be described theoretically, the δ(Zr) values of Cp_2ZrX_2 (X = Br, Cl, Me) **(1a−c)** have been computed with the IGLO-SCF and the GIAO-SCF methods. The hexahalogeno complexes ZrX_6^{2-} (X = F, Cl) have also been considered because they cover a somewhat larger chemical shift range. It is known for first-row compounds that optimized geometries often perform better in chemical shift calculations than do experimental structures.[26,27] This may not always be the case; for a consistent description, however, the IGLO and GIAO computations employed ab initio geometries optimized at a comparable theoretical level, SCF/B′.

As can be seen from the results in Table 5, the trend of $\delta(^{91}Zr)$ is well reproduced for the zirconocenes at IGLO-SCF/II and GIAO-SCF/II levels, over a range of ca. 500 ppm. Further increase of the basis set affects the computed δ values only slightly, up to ca. 10 ppm (compare the corresponding II and III′ entries in Table 5). The only case with larger deviations between theoretical and experimental data is ZrF_6^{2-}, for which also unusually large differences between the corresponding IGLO and GIAO values are apparent. Probably, even larger basis sets are required in this case to approach the SCF limit. Note that the inverse halogen effect, studied recently for Ti compounds in great detail,[85] is correctly reproduced computationally for $(C_5H_5)_2ZrCl_2$ **(1a)** and $(C_5H_5)_2ZrBr_2$ **(1b).**

Table 5. Ab Initio Computed ^{91}Zr Chemical Shifts for Zirconium Complexes[a]

	compd (sym)				
method	Cp_2ZrCl_2 (C_2)	$(C_5Me_5)_2ZrCl_2$ (C_s)	Cp_2ZrMe_2 (C_{2v})	ZrF_6^{2-} (O_h)	$ZrCl_6^{2-}$ (O_h)
IGLO-SCF/II	−87	37	434	−144	588
IGLO-SCF/III′	−91		435	−162	566
GIAO-SCF/II	−85	28	406	−12	612
GIAO-SCF/III′	−92		412	−66	601
exp	−112	85	386	−191[b]	601[c]

[a] δ values in ppm relative to Cp_2ZrBr_2 (C_2 symmetry); SCF/B′ geometries employed. [b] $[NH_4]_2[ZrF_6]/D_2O$. [c] $H_2[ZrCl_6]$/concentrated HCl.

Table 6. Principal Values of the ^{91}Zr Chemical Shift Tensors in Zirconocenes[a,b]

compd	δ_{11}	δ_{22}	δ_{33}	δ_{av}
Cp_2ZrCl_2 **(1a)**	−244	−182	+152	−91
Cp_2ZrBr_2 **(1b)**	−208	−138	+346	0
Cp_2ZrMe_2 **(1c)**	−180	−116	+1600	435

[a] In ppm relative to the isotropic value for Cp_2ZrBr_2, IGLO-SCF/III′ level. [b] Orientation of the principal axes: σ_{33} perpendicular to the ZrX_2 plane; σ_{22} along the 2-fold axis bisecting the XZrX′ angle; σ_{11} in the ZrX_2 plane perpendicular to σ_{11} and σ_{22}.

The principal values of the ^{91}Zr NMR chemical shift tensors in the zirconocenes $(C_5H_5)_2ZrX_2$ (X = Cl, Br, Me) are given in Table 6. The components δ_{11} and δ_{22} are always shielding and show only relatively small variations with X. Changes in δ_{33}, the component perpendicular to the ZrX_2 plane, are much larger, in particular when going to X = Me. The principal axis systems of the EFG tensors are oriented similarly as those of the chemical shift tensors; the direction of largest deshielding, δ_{33}, coincides with that of the largest absolute EFG, q_{zz}.

Except for ZrF_6^{2-}, the computed and experimental isotropic $\delta(^{91}Zr)$ chemical shifts agree reasonably well; the maximum deviation is 57 ppm for $(C_5Me_5)_2ZrCl_2$ (GIAO-SCF/II level, Table 5), and mean absolute deviations are on the order of 30 ppm, i.e. a few percent of the total ^{91}Zr chemical shift range (more than 1300 ppm). This performance is satisfactory, especially when bearing in mind that electron correlation and relativistic effects are neglected in the calculations. In addition, theoretical values for isolated molecules are compared to experimental data obtained in solution. Both the experimental ^{91}Zr chemical shift range and the relative sequence of the zirconocene derivatives are correctly reproduced at the SCF level. Thus, calculations at this level should allow reliable predictions of qualitative trends for ^{91}Zr chemical shifts.

One such trend, postulated by Böhme, Thiele, and Rufinska,[11] is the relationship between $\delta(^{91}Zr)$ and the CpZrCp′ angle, α; the Zr atom should be deshielded with increasing α, cf. the 125 ppm downfield shift in going from $(C_5H_5)_2ZrCl_2$ **(1a)** to $(C_5H_2$-1,2,4-^{i}Pr$_3)_2ZrCl_2$, which is paralleled by an opening of α by ca. 5°. When α is

(80) The difference of the latter value compared to that computed for **1a**, −0.2903 (Table 3), is a geometrical effect.

(81) Yoshida, T.; Koga, N.; Morokuma, K. *Organometallics* **1995**, *14*, 746.

(82) (a) Fan, L.; Harrison, D.; Woo, T. K.; Ziegler, T. *Organometallics* **1995**, *14*, 2018. (b) Lohreuz, J. C. W.; Woo, T. K.; Fan, L.; Ziegler, T. *J. Organomet. Chem.* **1995**, *497*, 91.

(83) Meier, R. J.; Doremaele, G. H. J. v.; Iarlori, S.; Buda, F. *J. Am. Chem. Soc.* **1994**, *116*, 7274.

(84) Ronova, I. A.; Alekseev, N. V. *Russ. J. Struct. Chem. (Engl. Transl.)* **1977**, *18*, 180.

(85) Berger, S.; Bock, W.; Frenking, G.; Jonas, V.; Müller, F. *J. Am. Chem. Soc.* **1995**, *117*, 3820.

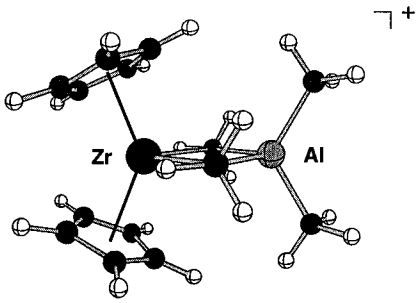

Figure 2. SCF/B′-optimized structure of the $[Cp_2ZrMe_2\text{-}AlMe_2]^+$ complex (**16**, C_{2v} symmetry imposed).

increased by as much as 15° in the SCF/B′ geometry of **1a**, indeed a downfield shift is computed for $\delta(^{91}Zr)$, albeit only by 14 ppm with respect to the undistorted structure. Closing α by 15° results in an increased, computed shielding by −23 ppm. As found for the EFGs (see above), tilting the Cp rings affects $\delta(^{91}Zr)$ much more: changing β by −7.5° and +7.5° affords computed $\Delta\delta(^{91}Zr)$ shifts of +14 and +78 ppm, respectively. Likewise, twisting both Cp rings by $\theta = 7.5°$ results in a computed downfield shift of $\Delta\delta(^{91}Zr)$ ca. +49 ppm. It therefore appears that ^{91}Zr chemical shifts depend on all geometrical parameters of the $(C_5H_5)_2Zr$ moiety and not just on the CpZrCp′ angle, α. In particular, $\delta(^{91}Zr)$ seems to be more sensitive to the Cp inclination and twist angles, β and θ, respectively. In contrast to the suggestions of Böhme et al., the theoretical ^{91}Zr chemical shifts are almost unaffected by the ClZrCl′ angle: changing this angle by +5 and −5° results in computed $\Delta\delta(^{91}Zr)$ shifts of only +4 and −1 ppm, respectively.

Another interesting aspect concerns the consequences of electron deficiency on the magnetic properties of cationic zirconocene complexes.[10] Species of the type $(C_5H_5)_2ZrR^+$ (R = alkyl) are believed to be the key intermediates in the catalytic olefin polymerization process.[2−5] It would be very interesting to probe the active catalyst by means of ^{91}Zr NMR spectroscopy, but $(C_5H_5)_2ZrR^+$ species are far too reactive to be observable on the NMR time scale. An electronic structure not unlike that of $(C_5H_5)_2ZrMe^+$ **(15)** may be preserved in complexes such as $(C_5H_5)_2ZrMe_2{\cdot}B(C_6F_5)_3$;[52] cf. the canonical resonance formulation as $[(C_5H_5)_2ZrMe]^+\text{-}[MeB(C_6F_5)_3]^-$. However, ^{91}Zr NMR signals could not be recorded for this or for similar complexes, presumably due to very large correlation times, τ_c.

According to the ab initio $\delta(^{91}Zr)$ value predicted for $(C_5H_5)_2ZrMe^+$ **(15)**, 698 ppm (GIAO-SCF/II level employing the SCF/B′ geometry, C_s symmetry imposed), the Zr atom is strongly deshielded in such cationic, unsaturated complexes. Even larger Zr chemical shifts are known, e.g. δ = 893 ppm for $Zr(NMe_2)_4$ **(14)**. In contrast, the metal is strongly shielded when multicenter bonding is involved: for $[(C_5H_5)_2ZrMe_2AlMe_2]^+$ **(16)**, formally a complex of **15** and $AlMe_3$ (Figure 2), a ^{91}Zr chemical shift of −12 ppm is computed (GIAO-SCF/II, C_{2v}-symmetric SCF/B′ geometry).

$[(C_5H_5)_2ZrMe_2AlMe_2]^+[B(C_6F_5)_4]^-$ **(16)** is reported to be stable at room temperature and is inactive as a polymerization catalyst.[86] The increase in Zr shielding predicted for this cationic complex with respect to neutral $(C_5H_5)_2ZrMe_2$ **(1c)** is noteworthy, $\Delta\delta$ ca. −400 ppm. In this context it is interesting to note that highly shielded transition metal complexes are often catalytically inactive.[87,88] The Zr atom is shielded even though two 2c−2e bonds are formally replaced by two 3c−2e bonds; i.e., electron density is actually removed from the Zr−C bonds. The strong shielding of $\delta(^{91}Zr)$ in **16** is paralleled by a decrease in the computed EFG: the q_{zz}^2(rel) value is only ca. half of that obtained for **1c**. Thus, the extent of the line broadening for **16** due to a larger τ_c should be significantly reduced because of the smaller EFG, and the $\delta(^{91}Zr)$ NMR signal could well be observable.

Conclusion

^{91}Zr Chemical shifts and line widths of ring-bridged and ring-substituted zirconocenes depend considerably on electronic and steric effects that can be adequately reproduced by ab initio computations. Signal detection is limited to complexes with line widths < 10 kHz, thus excluding the compounds of catalytic interest. Line widths $\Delta\nu_{1/2}$ are not solely determined by the correlation times, τ_c (and, thus, by the molecular size), but also by the magnitude of the electric field gradient, EFG, at the Zr atom. Ab initio computations suggest that the EFG is decisive for $\Delta\nu_{1/2}$ when the substituents at Zr are varied, e.g. in the series $(C_5H_5)_2ZrX_2$ (X = Br, Cl, Me) **(1a−c)**. Substituents at the Cp rings usually exert a much smaller effect on the computed EFGs at the Zr atom. As a consequence, the line widths should be dominated by τ_c in these cases, in accord with experimental observations.

Experimental trends in ^{91}Zr NMR chemical shifts of zirconocenes are well reproduced computationally employing IGLO-SCF or GIAO-SCF methods and large basis sets. Model calculations suggest that $\delta(^{91}Zr)$, as well as the EFGs, are quite sensitive to the structural parameters, in particular to the inclination and twist angles of the Cp rings, and, to a lesser extent, to the CpZrCp′ angle. A substantial deshielding, $\delta(^{91}Zr)$ ca. 700 ppm, is predicted for $(C_5H_5)_2ZrMe^+$ (**15**), the active olefin-polymerizing catalyst. In contrast, the Zr atom is strongly shielded in going to $[(C_5H_5)_2ZrMe_2AlMe_2]^+$ (**16**), formally a complex of **15** and $AlMe_3$, δ(calc) = −12 ppm.

Acknowledgment. This work has been supported by the Swiss National Science Foundation, the Fonds der Chemischen Industrie, BMFT, and the Volkswagen-Stiftung. G.H. wishes to thank Dr. W. Kozminski, Dr. D. Nanz, and Dr. A. Linden for helpful support. M.B. gratefully acknowledges generous support from W. Thiel. Calculations have been performed on IBM/RS 6000 workstations of the Organisch-chemisches Institut and of the Rechenzentrum der Universität Zürich. S.B. and H.H.B. thank Mr. T. Haselwander for providing crystals of $Me_4C_2(C_5H_4)_2ZrCl_2{\cdot}CHCl_3$.

Supporting Information Available: ORTEP diagrams and tables of X-ray parameters, atom coordinates, thermal parameters, and bond distances and angles (21 pages). Ordering information is given on any current masthead page.

OM950757C

(86) Bochmann, M.; Lancaster, S. J. *Angew. Chem., Int. Ed. Engl.* **1994**, *33*, 1634.
(87) Bender, B. R.; Koller, M.; Nanz, D.; von Philipsborn, W. *J. Am. Chem. Soc.* **1993**, *115*, 5889.
(88) Bönnemann, H.; Brijoux, W.; Brinkmann, R.; Meurers, W.; Mynott, R.; von Philipsborn, W.; Egolf, T. *J. Organomet. Chem.* **1984**, *272*, 231.
(89) The maximum uncertainty of the chemical shifts is ±10 ppm for broad lines.